Supplementary Section

Section 1

The Fowler-Nordheim function

We show in Table 1 the constants about the (*eq. 2*) with the flux of electrons ***J*** and the current emitted ***I*** from the sample for different electric field ***F (V/m)*** (Paulini et al. 1993)***.***

$$J(F,\phi) = \frac{q_1 F^{q_2}}{\phi^{q_3}\left(1+q_4\frac{\phi^{q_5}}{\phi^{q_3}(1+q_4\,F^{q_6})}\right)} \cdot exp^{\left(q_7\frac{\phi^{q_8}}{F^{q_9}}\right)} \quad (2)$$

q_1	7.3×10^{-6}
q_2	1.90593
q_3	0.810323
q_4	2.36641×10^{-22}
q_5	2.43459
q_6	5.22916
q_7	6.71665×10^{9}
q_8	1.49781
q_9	0.998795
q_{10}	197.477
q_{11}	0.205375
q_{12}	0.145045
ϕ (eV)	5 (*Nickel*)

F (V/m)	J (F, ϕ) (A/m²)	I (A)
1×10^{9}	1.3×10^{-22}	3.4×10^{-37}
2×10^{9}	2.2×10^{-5}	5.6×10^{-20}
3×10^{9}	1.7×10^{1}	4.3×10^{-14}
4×10^{9}	1.8×10^{4}	4.5×10^{-11}
5×10^{9}	1.2×10^{6}	3.2×10^{-9}
6×10^{9}	2.3×10^{7}	5.8×10^{-8}
7×10^{9}	1.9×10^{8}	4.9×10^{-7}
8×10^{9}	9.9×10^{8}	2.4×10^{-6}
9×10^{9}	3.6×10^{9}	9.0×10^{-6}
1×10^{10}	1.0×10^{10}	2.6×10^{-5}

Table 1: Electric field and current extract to the Fowler-Nordheim equation (1,2) with curvature radius of 20nm.

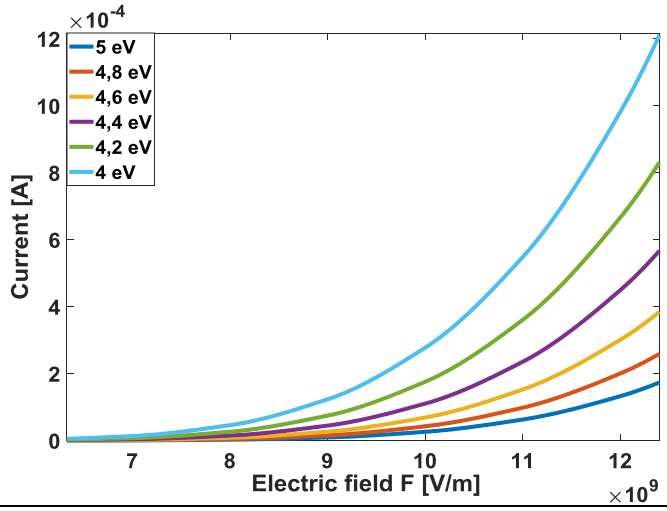

Fig. 17. *Current emitted from apex of APT sample with curvature radius R = 50nm for different work functions* $4eV < \phi < 5eV$ *and electric fields.*

We represent the exponential evolution of current emitted from apex of sample in Figure 17 for different electric field from Table 1.

Section 2

Damaged tungsten in field ion microscopy due to helium implantation

In Figure 18a and 18b we applied negative pulses of $2{,}000\,V$ and $2{,}200\,V$ on tungsten sample in He environment gas (P ~ 10^{-5} mbar). Multiple defects are observed within first 10 evaporated atomic layers. In the case of -$2000V$, we observe the creation of small interstitial groups and vacancies. In the case of 2,200 V negative pulses more important and numerous interstitial sites and vacancies with a cavity on the right in Figure 18 for 10 evaporated layers are observed. The defects generated due to the in-situ pulsed implantation are more important and visible at 10 evaporated atomic layers when we increase the negative voltage pulse applied to the sample. We note also the presence of larger interstitial groups. We can also specify that knowing the voltage at which the tip was evaporated and knowing the evaporation field of tungsten that we assume at $F = 52\,V.nm^{-1}$. The negative fields in the case of $2{,}000\,V$ and $2{,}200\,V$ are respectively estimated at $16\,and\,17\,V.nm^{-1}$. It's important to note that O.V Dudka, in his study with constant voltage was limited to $8\,V.nm^{-1}$, therefore, pulsed allows access to reach higher negative electric field.

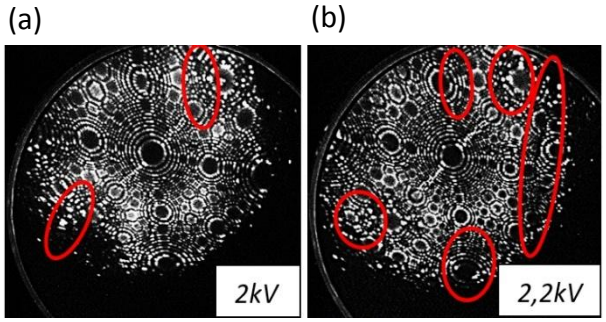

Fig. 18. *Images FIM of tungsten tip with Helium implantation (a) at 2,000 V and (b) at 2,200 V of negative pulse at 10 kHz during 5 minutes with 10 evaporated layers.*

Section 3

Study of the angles of hydrogen ions implanted at the tip apex.

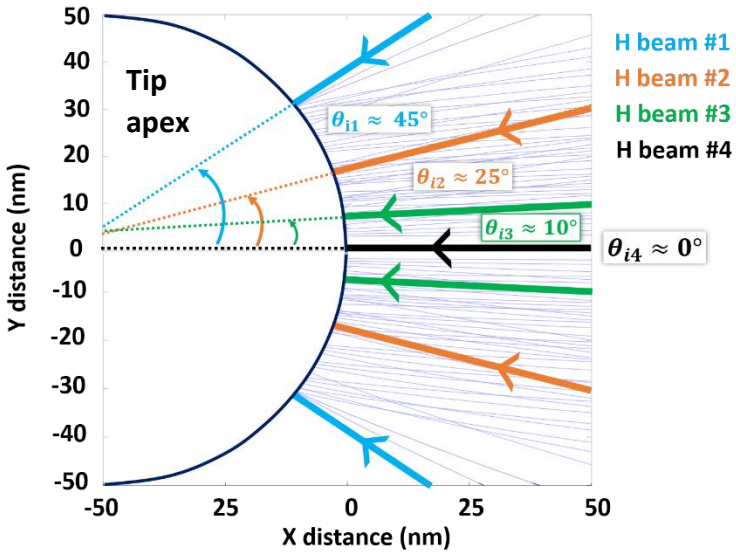

Fig. 19. *Trajectories of hydrogen ions implanted at the apex of APT sample with a study of their implantation angles relative to the sample normal for 4 H beams.*

We study 4 trajectories in particular represented by 4 colors in Figure 19. H beam #1 in blue represents the limit of possible angles for the hydrogen ions implantation in FOV instrument around 45° to the sample normal. Beams #2, #3, and #4 represented in orange, green, and black represent typical cases of implantation with angles that can vary from 0° to +30° to the sample normal.

This angle study thus allows us to consider the effects of channeling that may occur during implantation as negligible, because hydrogen ions will in any case collide with an atomic row very quickly as they penetrate the material deeply.